Hindawi
International Journal of Aerospace Engineering
Volume 2019, Article ID 6161032, 13 pages
https://doi.org/10.1155/2019/6161032

Research Article

Suboptimal Midcourse Guidance with Terminal-Angle Constraint for Hypersonic Target Interception

Shizheng Wan, Xiaofei Chang, Quancheng Li, and Jie Yan

School of Astronautics, Northwestern Polytechnical University, Xi'an, Shaanxi 710072, China

Correspondence should be addressed to Shizheng Wan; wshizheng2014@mail.nwpu.edu.cn

Received 17 November 2018; Revised 28 December 2018; Accepted 16 January 2019; Published 7 April 2019

Academic Editor: Seid H. Pourtakdoust

For the problem of hypersonic target interception, a novel midcourse guidance method with terminal-angle constraint is proposed. Referring to the air-breathing and the boost-gliding hypersonic targets, flight characteristics and difficulties of interception are analyzed, respectively. The requirements of midcourse guidance for interceptors are provided additionally. The kinematics model of adversaries is established concerning line-of-sight coupling in longitudinal and lateral planes. Suboptimal guidance law with terminal-angle constraint, specifically the final line-of-sight angle or impact angle, is presented by means of model predictive static programming. The trajectory is optimized and the load factor would finally converge after penalizing control sequence and output deviations. The realization of terminal angle is firstly verified with a constant speed target. A full interception scenario is further simulated focusing on a typical boost-gliding target, which flies along a skipping trajectory. Results show the success of providing handover conditions for intercepting hypersonic targets.

1. Introduction

The hypersonic vehicle, typically traveling greater than Mach 5 in the near space, has developed rapidly in recent years, and their weaponization has accelerated. Compared with conventional missiles, hypersonic weapons show great advantages of diverse launching platforms, fast flight speed, and strong penetration capability. Aiming at time-sensitive and high-value targets, they pose severe challenges to the traditional antiaircraft or antimissile defense system. Hypersonic vehicles are going through intensive flight testing, for instance, the "Hypersonic Air-breathing Weapon Concept" and "Tactical Boost Glide" [1], the Russian "Zircon" hypersonic cruise missile [2], and the Chinese "DF-ZF" hypersonic glide vehicle [3, 4]. The defense system should be upgraded and prepared to meet the requirements of the future battlefield.

In order to eliminate the target in time, modern interceptors generally require the ability of beyond-visual-range air combat. Midcourse guidance is vital to the entire interception process. The purpose is to lead the interceptor to a desired position, where not only the target can be acquired but also a good initial angle is obtained for the terminal phase, thus to increase the interception rate. Midcourse guidances for intercepting conventional aviation targets or ballistic missiles are relatively mature. For example, concerning air-to-air missile, singular perturbation theory was applied to the derivation of near-optimal midcourse guidance in articles [5–7], but they did not consider the angle alignment constraints. Focusing on the optimal guidance problem with angular constraint, Indig et al. [8] proposed an analytic guidance law with a linear dynamic model, which would cause control saturation at the time of interception. Liu et al. [9] designed a biased proportional navigation guidance method with attitude constraint and line-of-sight angle rate control, but it mainly aimed at stationary ground target, not to mention the capability of energy management. Taking constant acceleration into consideration, Seo and Tahk [10] provided a closed-loop midcourse guidance law, but the terminal constraint can be fulfilled only under the assumption that the impact point was precisely predicted. To maximize the kill probability, Phillips and Drake [11] designed a two-tier approach for surface-to-air midcourse trajectory with an auxiliary constraint on an intersection approach angle. Three classes of midcourse guidance laws, namely, optimal fuel,

optimal energy, and closed-loop explicit strategy, are proposed by Jalali-Naini and Pourtakdoust [12] with a zero-effort miss differential equation. Selecting different objectives and constraint functions, Reza and Abolghasem [13] solved an optimal interception problem with receding horizon control; commands are generated online by means of a differential flatness concept and nonlinear programming. Characterized by ultrafast speed and large-scale maneuverability, the requirements for hypersonic target interception become extremely strict, thus failing most of the existing midcourse guidance methods. New approaches must be found for these special targets, which can not only optimize trajectory online but also satisfy terminal-angle constraint.

To solve the real-time suboptimal problem with terminal constraints, Dwivedi et al. [14, 15] and Padhi and Kothari [16] put forward the model predictive static programming (MPSP) technique, which combines the "model predictive control" and "approximate dynamic programming" philosophies. With the qualities of accurate convergence and low computational cost, the MPSP technique has attracted extensive attention. Applying the MPSP algorithm, Oza and Padhi [17] presented a guidance law for air-to-ground missiles, which satisfies the constraint of terminal impact angle; superiority was demonstrated in comparison with augmented proportional navigation guidance and explicit linear optimal guidance. Halbe et al. [18] presented a robust suboptimal reentry guidance scheme for a reusable launch vehicle with the help of the MPSP algorithm. Apart from hard constraints of terminal conditions, soft constraints on path and control were also introduced through an innovative cost function, which consists of several components with various weighting factors. To solve the state variable inequality constraint, Bhitre and Padhi [19] converted the MPSP problem into an unconstrained but higher dimension one by means of a slack variable technique. Afterwards, the state constrained MPSP formulation was tested on an air-to-air engagement scenario. Considering the soft landing problem of a lunar craft during the powered descent phase, Sachan and Padhi [20] proposed a fuel optimal guidance law under the help of G-MPSP, where both terminal position and velocity were satisfied by adjusting the magnitude and angle of thrust. Bringing in sliding mode control, S. Li and X. Li [21] solved the divergence problem of the common MPSP algorithm caused by model inaccuracy; better robustness was proved when applied to maneuvering target interception. Moreover, Maity et al. [22, 23], Kumar et al. [24], and Guo et al. [25] also promoted the MPSP theory and applied it to the guidance design.

These aforementioned MPSP guidance laws in [15, 17] only lead the vehicle to a desired position defined by $Y(X)$ and $Z(X)$. However, when referring to a defense scenario, the optimal handover point changes with the maneuvering target, which requires additional prediction in every guidance cycle. In the process of midcourse guidance design for three-dimensional interception, the line-of-sight is not considered, which is vital to the flight trajectory and the startup of detection system. In addition, state-of-the-art guidance methods for intercepting hypersonic speed and large-scale maneuverable target are rarely researched to the best of the authors' knowledge. To solve these problems, this paper adopts the line-of-sight coupled interception model and proposes a novel midcourse guidance method with the MPSP technique according to the characteristics of a specific target, which can optimize the interceptor's trajectory and also meet the handover constraints.

The rest paper is organized as follows. In Section 2, the characteristics and technical requirements of midcourse guidance for hypersonic target interception are analyzed, and a three-dimensional interception model is established. In Section 3, suboptimal guidance law with constrained terminal line-of-sight or impact angle is derived utilizing the MPSP approach. The guidance scheme is validated in Section 4, considering a constant speed target and a typical boost-gliding target. Finally, the text is briefly summarized in Section 5.

2. Midcourse Guidance Problem

2.1. Consideration for Hypersonic Interceptor. Referring to the hypersonic target, many aspects must be taken into consideration while designing the interceptor's midcourse guidance.

(1) Different from most ballistic missiles, hypersonic target can perform a wide range of maneuver strategies without affecting the final attack performance during the strike mission, which raises the demand of accuracy and timeliness for target tracking and prediction

(2) Limited by the working condition of structure and detection system, the interceptor's speed is generally slower than that of the target's. Therefore, head-on or head pursuit guidance [26, 27] remains the only choice

(3) In view of the high closing speed and the capability of penetration, the velocity heading error must be small enough at the beginning of the terminal phase. Head-on condition is beneficial for a successful interception

(4) As the hypersonic target flies in a large airspace and midcourse guidance takes a relatively long time, the abilities of rapid trajectory correction and flight energy management become essential for the interceptor

Hypersonic vehicles are mainly classified into two categories, the air-breathing type equipped with scramjet engine like the X-51 and the boost-gliding type powered by rockets like the HTV-2 [28]. Significant differences can be found in their maneuvering strategy and capability. The air-breathing hypersonic target is critically restricted by the operation conditions of the scramjet. It generally adopts horizontal flight in the longitudinal plane during cruise segment, while bank-to-turn control is applied in the lateral plane to achieve evasive maneuvers. Being absent of thrust after reentry, the boost-gliding target however employs skip ballistic to increase flight distance; bank angle is adjusted to ensure the heading direction. Target identification can be done with the help of early warning systems. Midcourse guidance is then designed, respectively, according to the differences between air-breathing and boost-gliding hypersonic targets.

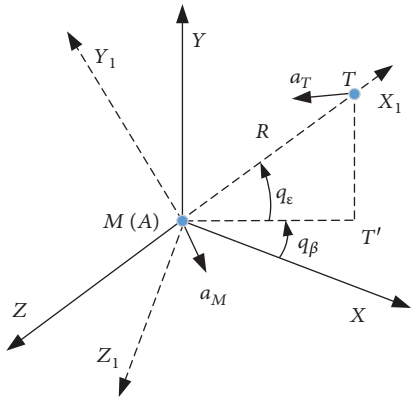

Figure 1: Interceptor and target relationship.

Based on the above analyses, the instructions of the midcourse guidance design for the hypersonic target interceptor are as follows:

(1) To make use of the "zero-effort miss" concept, the line-of-sight rate had better approach zero at the handover of the midcourse phase and terminal phase. So long as the target does not maneuver, the interceptor will strike on the target without extra control. In other words, the load factor of the interceptor tends to zero, which is beneficial to the separation from the booster and the overload reservation for compensating target perturbations

(2) To satisfy the capture conditions of the on-board seeker and improve the success rate of final interception, it is important to meet the limit of the final line-of-sight angle or impact angle. The optimal interception geometry will be obtained if an approximate head-on scenario is realized

(3) Considering the trajectory smoothness and energy constraint, the control command for the interceptor should be optimized

(4) For the target implementing a large maneuver, its flight path angle or velocity azimuth angle changes frequently; midcourse guidance with velocity angle alignment for the interceptor becomes overreacting and guidance performance will suffer. In such circumstances, line-of-sight constrained midcourse guidance is preferred to realize the optimal aspect angle. Otherwise, guidance laws with a velocity angle constraint will be better if the target employs a small maneuver. In this way, the optimized impact angle can be achieved [29], thus reducing the overload demand for the terminal phase

2.2. Coupled Line-of-Sight Dynamics. The kinematic relationship between the pursuer and evader in a three-dimensional space is shown in Figure 1, where M and T are centroids of the interceptor and target, respectively. $MX_1Y_1Z_1$ is the line-of-sight coordinate system. The axis MX_1 is aligned with the line-of-sight and points to target T. Staying in a vertical plane, the axis MY_1 is normal to MX_1 and points upward. The axis MZ_1 is defined by the right-hand rule and is normal to MX_1 and MY_1. $AXYZ$ is the inertial reference coordinate system, and for clarity of illustration, its origin A is translated to coincide with the origin M. Hereafter, two Euler angles are introduced [30]. q_ε stands for the elevation line-of-sight, namely, the angle between the line-of-sight and horizontal plane ZAX. q_β is the azimuth line-of-sight, which acts on the horizontal plane with respect to reference direction AX. R represents the relative distance between the interceptor and target.

The unit vectors of the inertial reference coordinate $AXYZ$ and the line-of-sight coordinate $MX_1Y_1Z_1$ are $(\mathbf{i}, \mathbf{j}, \mathbf{k})$ and $(\mathbf{i}_1, \mathbf{j}_1, \mathbf{k}_1)$, respectively. Transformation from $MX_1Y_1Z_1$ to $AXYZ$ can be done within two steps: clockwise rotate q_ε angle with respect to axis MZ_1 and then clockwise rotate q_β angle with respect to axis MY_1. In this way, we get

$$\begin{bmatrix} \mathbf{i} \\ \mathbf{j} \\ \mathbf{k} \end{bmatrix} = L\left(q_\varepsilon, q_\beta\right) \begin{bmatrix} \mathbf{i}_1 \\ \mathbf{j}_1 \\ \mathbf{k}_1 \end{bmatrix}, \tag{1}$$

where the transformation matrix is expressed as

$$\begin{aligned} L\left(q_\varepsilon, q_\beta\right) &= \begin{bmatrix} \cos q_\beta & 0 & \sin q_\beta \\ 0 & 1 & 0 \\ -\sin q_\beta & 0 & \cos q_\beta \end{bmatrix} \begin{bmatrix} \cos q_\varepsilon & -\sin q_\varepsilon & 0 \\ \sin q_\varepsilon & \cos q_\varepsilon & 0 \\ 0 & 0 & 1 \end{bmatrix} \\ &= \begin{bmatrix} \cos q_\beta \cos q_\varepsilon & -\cos q_\beta \sin q_\varepsilon & \sin q_\beta \\ \sin q_\varepsilon & \cos q_\varepsilon & 0 \\ -\sin q_\beta \cos q_\varepsilon & \sin q_\beta \sin q_\varepsilon & \cos q_\beta \end{bmatrix}. \end{aligned} \tag{2}$$

After then, the rotation angular velocity $\boldsymbol{\omega}$ of the line-of-sight coordinate relative to the inertial reference coordinate is obtained by

$$\boldsymbol{\omega} = \dot{q}_\beta \mathbf{j} + \dot{q}_\varepsilon \mathbf{k}_1 = \dot{q}_\beta \sin q_\varepsilon \mathbf{i}_1 + \dot{q}_\beta \cos q_\varepsilon \mathbf{j}_1 + \dot{q}_\varepsilon \mathbf{k}_1. \tag{3}$$

The range vector in the line-of-sight coordinate is $\mathbf{R}$ $[R, 0, 0]^{\mathrm{T}}$. Applying the vector derivative method, the relative velocity between the interceptor and the target is given as

$$\mathbf{V} = \dot{R}\mathbf{i}_1 + \boldsymbol{\omega} \times R\mathbf{i}_1 = \dot{R}\mathbf{i}_1 + R\dot{q}_\varepsilon \mathbf{j}_1 - R\dot{q}_\beta \cos q_\varepsilon \mathbf{k}_1. \tag{4}$$

Considering nonlinear point mass dynamics, the acceleration vectors of the interceptor and target on the line-of-sight coordinate system are denoted as $\mathbf{a}_M = [a_{MR}, a_{M\varepsilon}, a_{M\beta}]^{\mathrm{T}}$ and $\mathbf{a}_T = [a_{TR}, a_{T\varepsilon}, a_{T\beta}]^{\mathrm{T}}$, respectively. Applying the vector derivative method once again to relative velocity gives

$$\mathbf{a}_T - \mathbf{a}_M = \boldsymbol{\omega} \times \mathbf{V} + \frac{\partial \mathbf{V}}{\partial t}. \tag{5}$$

Substituting (3) and (4) to (5) and rearranging equations, the line-of-sight coupled 3D interception model is obtained:

$$\begin{aligned} a_{TR} - a_{MR} &= \ddot{R} - R\dot{q}_\varepsilon^2 - R\dot{q}_\beta^2 \cos^2 q_\varepsilon, \\ a_{T\varepsilon} - a_{M\varepsilon} &= R\ddot{q}_\varepsilon + 2\dot{R}\dot{q}_\varepsilon + R\dot{q}_\beta^2 \sin q_\varepsilon \cos q_\varepsilon, \\ a_{T\beta} - a_{M\beta} &= -R\ddot{q}_\beta \cos q_\varepsilon - 2\dot{R}\dot{q}_\beta \cos q_\varepsilon + 2R\dot{q}_\varepsilon\dot{q}_\beta \sin q_\varepsilon. \end{aligned} \tag{6}$$

Generally, the thrust magnitude of the interceptor is designed previously according to the velocity characteristics, and the drag on the vehicle is closely related to its dynamic pressure. As a consequence, the term a_{MR} is difficult to be controlled during flight. In fact, like proportional navigation (PN) and most other guidance laws do, the control of a_{MR} is not necessary as long as $\dot{R} < 0$. Thereby, the equation along the MX_1 direction can be ignored.

Defining the state variables $x_1 = q_\varepsilon$, $x_2 = \dot{q}_\varepsilon$, $x_3 = q_\beta$, and $x_4 = \dot{q}_\beta$, the state transition equation for the line of sight and its rate can be written as

$$\begin{aligned} \dot{x}_1 &= x_2, \\ \dot{x}_2 &= -\frac{2\dot{R}}{R}x_2 - x_4^2 \sin x_1 \cos x_1 - \frac{a_{M\varepsilon}}{R} + \frac{a_{T\varepsilon}}{R}, \\ \dot{x}_3 &= x_4, \\ \dot{x}_4 &= -\frac{2\dot{R}}{R}x_4 + 2x_2x_4 \tan x_1 + \frac{a_{M\beta}}{R\cos x_1} - \frac{a_{T\beta}}{R\cos x_1}. \end{aligned} \tag{7}$$

The objective in the midcourse guidance design is to optimize the control history of $a_{M\varepsilon}$ and $a_{M\beta}$, meanwhile satisfying the constraints in the guidance process and at the handover.

3. Angle Constrained MPSP Guidance

In this section, the suboptimal midcourse guidance law with a terminal-angle constraint is derived by means of the MPSP algorithm, in particular, the line-of-sight constrained MPSP guidance and the impact angle constrained MPSP guidance.

3.1. Line-of-Sight Constrained Guidance. A brief principle of MPSP can be described as follows. Firstly, expand the observed output with first-order Taylor series at the expected terminal point. Then, the deviation between the predicted output and the desired value can be formulated by an initial state error and control error history. Applying an appropriate cost function, the corrected control is derived from iterative calculation, when the final output value approximates the expected one.

Because of the guidance iteration, flight trajectory is corrected in each cycle to get rid of external disturbance. The following assumptions are acceptable while processing the guidance design:

(1) Different from the terminal phase, midcourse guidance lasts longer. The hypersonic target is most likely to adopt various maneuver strategies, causing the changes of its acceleration at all times. It is not reliable to predict the future maneuvers of the hypersonic target. Therefore, the acceleration is neglected briefly

(2) Applying the quasisteady assumption, the closing velocity of the adversaries is regarded as a constant, namely, $\dot{R} = -V_c$. Guidance law acts periodically, the closing velocity is updated in every guidance cycle, and the deviations would be corrected

Discretizing the plant dynamics (7) with Euler's integration formula gives

$$\mathbf{X}_{k+1} = \mathbf{F}_k(\mathbf{X}_k, \mathbf{U}_k) = \mathbf{X}_k + f(\mathbf{X}_k, \mathbf{U}_k)T, \tag{8}$$

where $\mathbf{X} \in \mathbb{R}^4$, $\mathbf{U} \in \mathbb{R}^2$, subscript $k = 1, 2, \ldots, N$ is the time index, and T is the step size.

Assuming that the interceptor can receive immediate position (x_T, y_T, z_T) and velocity (V_{xT}, V_{yT}, V_{zT}) of the target from remote data-link during the midcourse, together with its position (x_M, y_M, z_M) and velocity (V_{xM}, V_{yM}, V_{zM}) from an on-board IMU system, the relative position and velocity can be obtained by

$$\begin{aligned} \mathbf{r} &= [x_{MT}, y_{MT}, z_{MT}]^{\mathrm{T}} \\ &= [x_T - x_M, y_T - y_M, z_T - z_M]^{\mathrm{T}}, \\ \mathbf{V} &= \left[V_{xMT}, V_{yMT}, V_{zMT}\right]^{\mathrm{T}} \\ &= \left[V_{xT} - V_{xM}, V_{yT} - V_{yM}, V_{zT} - V_{zM}\right]^{\mathrm{T}}. \end{aligned} \tag{9}$$

Therefore, the line-of-sight information is derived as

$$\begin{aligned} q_\varepsilon &= \arctan \frac{y_{MT}}{\sqrt{(x_{MT})^2 + (z_{MT})^2}}, \\ \dot{q}_\varepsilon &= \frac{x_{MT}V_{yMT} - y_{MT}V_{xMT}}{(x_{MT})^2 + (y_{MT})^2 + (z_{MT})^2}, \\ q_\beta &= \arctan\left(-\frac{z_{MT}}{x_{MT}}\right), \\ \dot{q}_\beta &= \frac{z_{MT}V_{xMT} - x_{MT}V_{zMT}}{(x_{MT})^2 + (y_{MT})^2 + (z_{MT})^2}. \end{aligned} \tag{10}$$

Now, the measured output $\mathbf{Y} = [q_\varepsilon, \dot{q}_\varepsilon, q_\beta, \dot{q}_\beta]^{\mathrm{T}} \in \mathbb{R}^4$ is selected in terms of specific guidance requirements, right in the state of the system, and we get $\mathbf{Y}_k = \mathbf{X}_k$. Marking N as the prediction horizon of the MPSP method, the missile-target range step is expressed as $R_{\mathrm{step}} = (R_{\mathrm{init}} - \mathrm{R}_{\mathrm{end}})/(N-1)$, where R_{init} indicates the missile-target distance at every guidance epoch and R_{end} means the handover distance. Then, the increment of time is obtained by $T = R_{\mathrm{step}}/V_c$.

Through appropriate control modification $d\mathbf{U}$, MPSP drives the predicted terminal output $\mathbf{Y}_N$ to the expected value $\mathbf{Y}_N^*$. In consideration of the final line-of-sight constraints and parallel approach method, the desired output is select as

$$\mathbf{Y}_N^* = \left[q_{\varepsilon f}^*, 0, q_{\beta f}^*, 0\right]^{\mathrm{T}}. \tag{11}$$

Applying the Taylor series expansion to $\mathbf{Y}_N$ at the point $\mathbf{Y}_N^*$ and ignoring higher-order terms, the output deviation is written as

$$d\mathbf{Y}_N = \left[\frac{\partial \mathbf{Y}_N}{\partial \mathbf{X}_N}\right] d\mathbf{X}_N, \tag{12}$$

where

$$\frac{\partial \mathbf{Y}_N}{\partial \mathbf{X}_N} = \begin{bmatrix} 1 & 0 & 0 & 0 \\ 0 & 1 & 0 & 0 \\ 0 & 0 & 1 & 0 \\ 0 & 0 & 0 & 1 \end{bmatrix}. \tag{13}$$

The transfer function of the state error can be derived from (8):

$$d\mathbf{X}_{k+1} = \left[\frac{\partial \mathbf{F}_k}{\partial \mathbf{X}_k}\right] d\mathbf{X}_k + \left[\frac{\partial \mathbf{F}_k}{\partial \mathbf{U}_k}\right] d\mathbf{U}_k. \tag{14}$$

In the formula, $d\mathbf{X}_k$ and $d\mathbf{U}_k$ represent the state error and control error at the k step, respectively; the partial derivatives of the state variables and the control variables are expressed as

$$\begin{aligned} \frac{\partial \mathbf{F}_k}{\partial \mathbf{X}_k} &= \begin{bmatrix} 1 & T & 0 & 0 \\ a_{21} & a_{22} & 0 & a_{23} \\ 0 & 0 & 1 & T \\ a_{41} & a_{42} & 0 & a_{44} \end{bmatrix}, \\ \frac{\partial \mathbf{F}_k}{\partial \mathbf{U}_k} &= \begin{bmatrix} 0 & 0 \\ b_{21} & 0 \\ 0 & 0 \\ 0 & b_{42} \end{bmatrix}, \end{aligned} \tag{15}$$

where

$$\begin{cases} a_{21} = -x_{4k}^2 \cos(2x_{1k})T, \\ a_{22} = 1 + 2V_c T/R_k, \\ a_{24} = -x_{4k} \sin(2x_{1k})T, \\ a_{41} = \left(\dfrac{2x_{2k}x_{4k}}{\cos^2(x_{1k})} + \dfrac{a_{M\beta k} \tan(x_{1k})}{R_k \cos(x_{1k})}\right)T, \\ a_{42} = 2x_{4k} \tan(x_{1k})T \\ a_{44} = 1 + 2V_c T/R_k + 2x_{2k} \tan(x_{1k})T, \\ b_{21} = -T/R_k, \\ b_{42} = T/(R_k \cos(x_{1k})). \end{cases} \tag{16}$$

Taking the step $k = N - 1$ in (14) and substituting it to (12), we obtain

$$d\mathbf{Y}_N = \left[\frac{\partial \mathbf{Y}_N}{\partial \mathbf{X}_N}\right] \left(\left[\frac{\partial \mathbf{F}_{N-1}}{\partial \mathbf{X}_{N-1}}\right] d\mathbf{X}_{N-1} + \left[\frac{\partial \mathbf{F}_{N-1}}{\partial \mathbf{U}_{N-1}}\right] d\mathbf{U}_{N-1} \right). \tag{17}$$

In this way, the output deviation is expressed as a function of the initial state error and control error sequences.

$$d\mathbf{Y}_N = \mathbf{A} d\mathbf{X}_1 + \mathbf{B}_1 d\mathbf{U}_1 + \cdots + \mathbf{B}_{N-1} d\mathbf{U}_{N-1}, \tag{18}$$

wherein the matrix $\mathbf{A}$ and the sensitivity matrices $\mathbf{B}_k$ are defined as

$$\begin{aligned} \mathbf{A} &= \left[\frac{\partial \mathbf{Y}_N}{\partial \mathbf{X}_N}\right] \left[\prod_{m=1}^{N-1} \frac{\partial \mathbf{F}_m}{\partial \mathbf{X}_m}\right], \\ \mathbf{B}_k &= \left[\frac{\partial \mathbf{Y}_N}{\partial \mathbf{X}_N}\right] \left[\prod_{m=k+1}^{N-1} \frac{\partial \mathbf{F}_m}{\partial \mathbf{X}_m}\right] \left[\frac{\partial \mathbf{F}_k}{\partial \mathbf{U}_k}\right]. \end{aligned} \tag{19}$$

Given the initial condition of the missile-target confrontation, no error exists in the first state, i.e., $d\boldsymbol{X}_1 = 0$, equation (18) yields

$$d\mathbf{Y}_N = \mathbf{B}_1 d\mathbf{U}_1 + \cdots + \mathbf{B}_{N-1} d\mathbf{U}_{N-1} = \sum_{k=1}^{N-1} \mathbf{B}_k d\mathbf{U}_k. \tag{20}$$

The sensitivity matrices $\mathbf{B}_k$ can be solved recursively in the following manner:

$$\begin{aligned} \mathbf{B}_{N-1}^0 &= \left[\frac{\partial \mathbf{Y}_N}{\partial \mathbf{X}_N}\right], \\ \mathbf{B}_k^0 &= \mathbf{B}_{k+1}^0 \left[\frac{\partial \mathbf{F}_{k+1}}{\partial \mathbf{X}_{k+1}}\right], \\ \mathbf{B}_k &= \mathbf{B}_k^0 \left[\frac{\partial \mathbf{F}_k}{\partial \mathbf{U}_k}\right]. \end{aligned} \tag{21}$$

To optimize the trajectory of the interceptor and maintain a smooth flight, define the quadratic objective function as

$$J = \frac{1}{2} \sum_{k=1}^{N-1} \left(\mathbf{U}_k^0 - d\mathbf{U}_k\right)^T \mathbf{R}_k \left(\mathbf{U}_k^0 - d\mathbf{U}_k\right), \tag{22}$$

where $\mathbf{R}_k$ is the positive definite weighting matrix and $\mathbf{U}_k^0$ is the previous control solution. Note that the weight matrix is alternatively chosen to adjust the magnitude of the control history at different time steps.

For the constrained optimal problem defined in equations (20) and (22), static optimization theory is applied, which gives the augmented cost function

$$\begin{aligned} J' = &\frac{1}{2} \sum_{k=1}^{N-1} \left(\mathbf{U}_k^0 - d\mathbf{U}_k\right)^T \mathbf{R}_k \left(\mathbf{U}_k^0 - d\mathbf{U}_k\right) \\ &+ \lambda^T \left(d\mathbf{Y}_N - \sum_{k=1}^{N-1} \mathbf{B}_k d\mathbf{U}_k\right). \end{aligned} \tag{23}$$

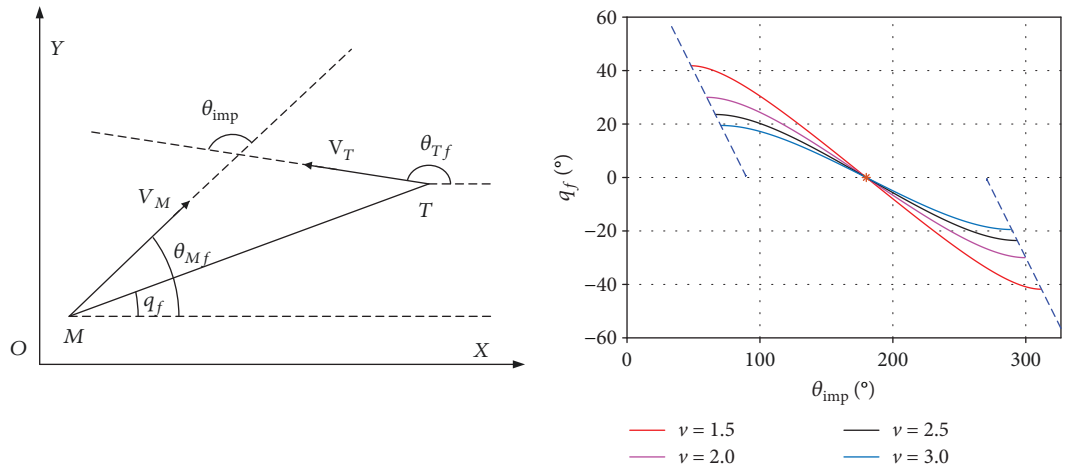

(a) Impact triangle

(b) θ_{imp} and q_f relationship

Figure 2: Interception angle in a 2D plane.

The necessary conditions for minimal J' are given by

$$\begin{aligned}\frac{\partial J_k'}{\partial d\mathbf{U}_k} &= -\mathbf{R}_k\left(\mathbf{U}_k^0 - d\mathbf{U}_k\right) - \mathbf{B}_k^T\lambda = 0,\\ \frac{\partial J_k'}{\partial \lambda} &= d\mathbf{Y}_N - \sum_{k=1}^{N-1}\mathbf{B}_k d\mathbf{U}_k = 0.\end{aligned} \tag{24}$$

Solving for the corrected control $\mathbf{U}_k$, we get

$$\mathbf{U}_k = U_k^0 - d\mathbf{U}_k = \mathbf{R}_k^{-1}\mathbf{B}_k^T A_\lambda^{-1}\left(d\mathbf{Y}_N - \mathbf{b}_\lambda\right), \tag{25}$$

where

$$\begin{aligned}\mathbf{A}_\lambda &= \left[-\sum_{k=1}^{N-1}\mathbf{B}_k\mathbf{R}_k^{-1}\mathbf{B}_k^T\right],\\ \mathbf{b}_\lambda &= \left[\sum_{k=1}^{N-1}\mathbf{B}_k\mathbf{U}_k^0\right].\end{aligned} \tag{26}$$

In conclusion, the line-of-sight constrained MPSP guidance is numerically solved by the control (25), considering the discrete guidance problem (8) with the required output (11) and cost function (22). Note that the control sequence $\mathbf{U}_k(k = 1, 2, \ldots, N-1)$ is solved in each guidance period, but only $\mathbf{U}_1$ is employed as the current guidance command. The suboptimal midcourse guidance law for target interception not only optimizes the flight control but also satisfies the terminal constraints of the line-of-sight angle and its rate.

3.2. Impact Angle Constrained Guidance. As already mentioned in Section 2.1, the midcourse guidance with velocity angle alignment exhibits better handover properties if the target's maneuver is somehow weak. However, only the line of sight and line-of-sight rate are involved while modeling the interception scenario. A solution can be found in [31], where the desired impact angle is able to be transferred into the final line-of-sight angle. For simplicity, the following process is done in the longitudinal plane and the lateral plane is similar.

The impact angle is defined as the angle between velocity vectors of the adversaries; particularly, we have

$$\theta_{\text{imp}} = \theta_T - \theta_M, \tag{27}$$

where θ_{imp} is the impact angle in the longitudinal plane and θ_T and θ_M are the flight path angles of the target and interceptor, respectively. A perfect head-on interception scenario is formed by restricting $\theta_{\text{imp}} = \pi$.

When the midcourse guidance comes to the end, the line-of-sight rate $\dot{q}$ has been driven to zero. The interceptor and target stay on an impact triangle geometry, as shown in Figure 2(a). Under this circumstance, the zero-effort miss can be guaranteed if both the interceptor and the target do not execute any further maneuvers from the instant time onward. Then, the relationship between the terminal line-of-sight angle and impact angle is given by

$$V_T \sin\left(\theta_{Tf} - q_f\right) - V_M \sin\left(\theta_{Mf} - q_f\right) = 0, \tag{28}$$

where V_T and V_M are the velocities of the hypersonic target and interceptor, respectively, q stands for the line-of-sight in a 2D plane, and subscript f represents the final value in midcourse guidance.

Noting the target-to-missile speed ratio $\nu = V_T/V_M$, rearranging (28) yields

$$q_f = \theta_{Tf} - \arctan\left(\frac{\sin\theta_{\text{imp}}}{\cos\theta_{\text{imp}} - \nu}\right) - n\pi. \tag{29}$$

Different from the situation in [31], the interceptor no longer has velocity advantage, namely, $\nu > 1$; the singular problem is structurally avoided. One-to-one condition of q_f and θ_{imp} is further analyzed, in which a monotonous zone including head-on condition can be found. Considering an

incoming target with $\theta_{Tf} = \pi$, the relationship between q_f and θ_{imp} changes according to the speed ratio ν, as shown in Figure 2(b). Since q_f is continuous, extreme points can be obtained by driving $dq_f/d\theta_{\text{imp}} = 0$, which gives $\nu \cos \theta_{\text{imp}} = 1$. In conclusion, for any desired impact angle $\theta_{\text{imp}} \in (\arccos(1/\nu), 2\pi - \arccos(1/\nu))$, a corresponding q_f can be calculated by (29).

Applying (29), the aforementioned line-of-sight constrained MPSP guidance is transferred into the impact angle constrained MPSP guidance, which actually constrains the final flight path angle for the interceptor in the midcourse phase. Note that the prediction of the target's terminal flight path angle is required.

4. Simulation

Three different scenarios are presented to validate the effectiveness of the constrained MPSP midcourse guidance law. The first two scenarios refer to the cruising hypersonic target with a constant velocity in the longitudinal plane. Line-of-sight constrained and impact angle constrained midcourse guidance are applied, respectively; The last scenario considers the gliding target with a skipping trajectory in a three-dimensional space, and a full guidance scheme including midcourse is adopted.

4.1. Problem Setup

4.1.1. Interceptor and Target Model. The interceptor is modeled using three-degree-of-freedom (3DOF) particle dynamics [15].

$$\begin{cases} \dot{x} = V\cos\theta\cos\psi, \\ \dot{y} = V\sin\theta, \\ \dot{z} = V\cos\theta\sin\psi, \\ \dot{V} = \dfrac{T-D}{m} - g\sin\theta, \\ \dot{\theta} = \dfrac{1}{V}\left(a_y - g\cos\theta\right), \\ \dot{\psi} = \dfrac{a_z}{V\cos\theta}, \\ \dot{m} = \dfrac{T}{I_{\text{sp}}}, \end{cases} \tag{30}$$

where x, y, and z are the positions of the interceptor, V is the vehicle speed, and m stands for mass. The relative flight path angle and velocity azimuth angle are θ and ψ, respectively; a_y and a_z represent the acceleration commands in the longitudinal and lateral planes; T and D donate the thrust and drag on the interceptor; and I_{sp} is the specific impulse of the rocket or reaction control system (RCS).

Taking conventional gliding vehicle interception as an example, the target adopts bank angle constrained predictor-corrector reentry guidance [32]. The particle dynamics of a common aero vehicle (CAV) over a nonrotating spherical earth model are applied, where the Coriolis and centrifugal inertial force are technically ignored.

Table 1: Convergence results of LOS constrained guidance.

		$R(m)$	$q_f(^\circ)$	$\dot{q}(\text{rad}/s)$	$n_{yf}(g)$
$q_f = -5^\circ$	Default	60000	-5	0	-0.149
	Real	59960	-5.000	$-5.908e-5$	
$q_f = 0^\circ$	Default	60000	0	0	-0.052
	Real	59972	$-8.377e-6$	$-1.800e-5$	
$q_f = 5^\circ$	Default	60000	5	0	-0.057
	Real	59940	5.000	$-2.21e-6$	

$$\begin{cases} \dot{r} = V\sin\theta, \\ \dot{\lambda} = \dfrac{V\cos\theta\sin\psi}{r\cos\phi}, \\ \dot{\phi} = \dfrac{V\cos\theta\cos\psi}{r}, \\ \dot{V} = -\dfrac{D}{m} - g\sin\theta, \\ \dot{\theta} = \dfrac{L\cos\sigma}{mV} + \left(\dfrac{V^2}{r} - g\right)\dfrac{\cos\theta}{V}, \\ \dot{\psi} = \dfrac{L\sin\sigma}{mV\cos\theta} + \dfrac{V}{r}\cos\theta\sin\psi\tan\phi, \end{cases} \tag{31}$$

where r is the radial distance from the earth's center to the gliding vehicle; λ and ϕ are the longitude and latitude of the location; and V is the vehicle speed. The flight path angle and velocity azimuth angle are marked as θ and ψ; L and D indicate the aerodynamic lift and drag; and σ is the controlled bank angle.

4.1.2. Overall Guidance Scheme. In order to improve mobility and timeliness of the interceptor platform, meanwhile expanding the defensive area, the air-launched interceptor is adopted. The ability of attack beyond visual range is vital to a multiple-layer intercept. Taking limited energy and load factor into account, the interceptor prefers a parabola trajectory for its boost guidance. In this phase, the interceptor separates from the air platform and climbs to the required altitude. The drag can be significantly reduced in a high altitude and its operational range is extended thereafter. The trigonometric guidance command [33] is applied for the smooth shifting from separation; thus, the overload would increase gently as expected. The flight path angle command and velocity azimuth angle command are given by

$$\begin{aligned} \dot{\theta}_M &= \frac{\pi}{2t_0}\theta_{\text{opt}}\sin\frac{\pi}{2}\frac{t}{t_0}, \\ \dot{\psi}_M &= \frac{\pi}{2t_0}\psi_{\text{opt}}\sin\frac{\pi}{2}\frac{t}{t_0}, \end{aligned} \tag{32}$$

where t represents the guidance time after separation, while t_0 is the total time preset for the initial phase; θ_{opt}

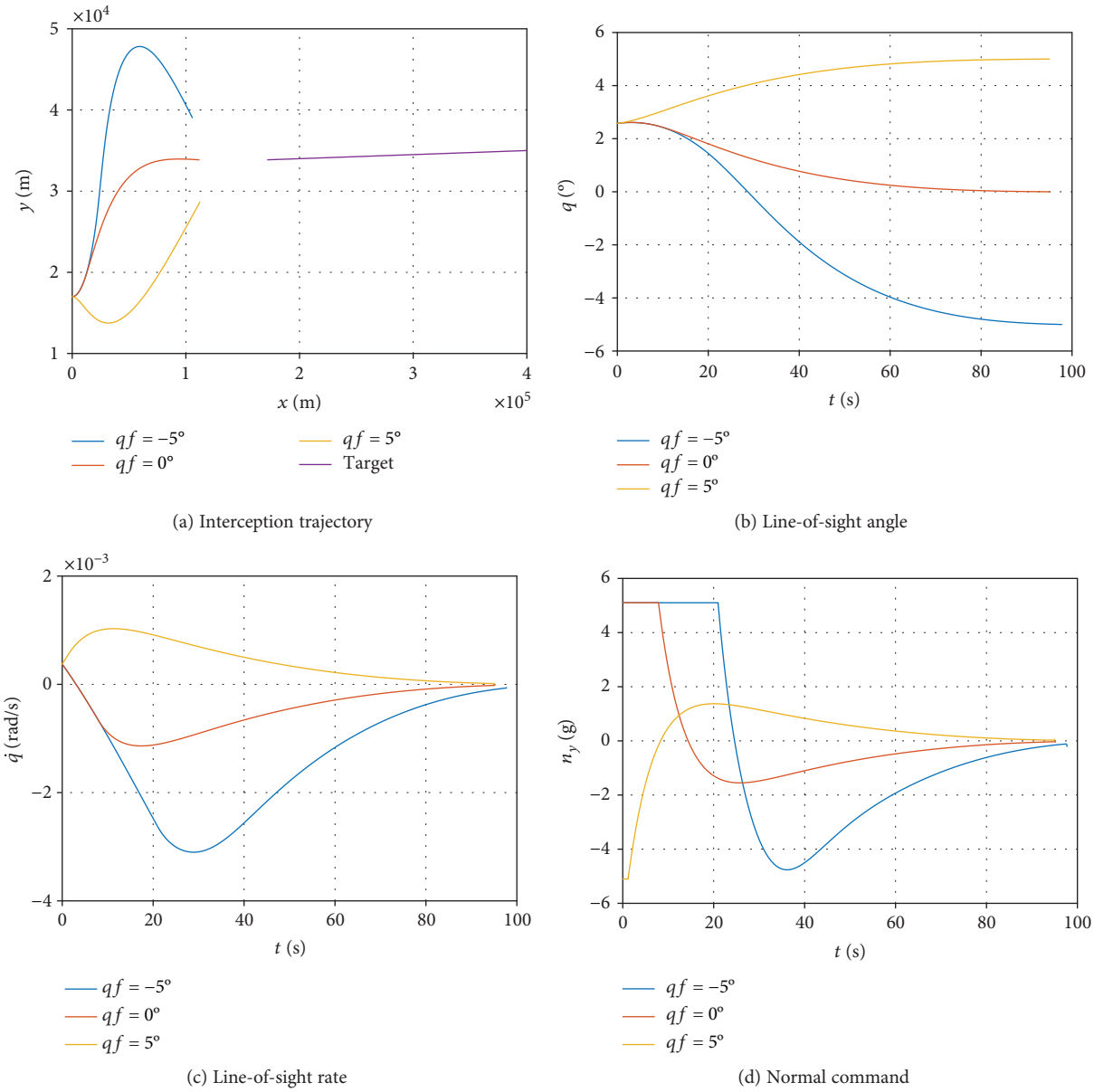

Figure 3: Simulation results of LOS constrained guidance.

and ψ_{opt} are the expected flight path angle and velocity azimuth angle depending on the predicted impact point and maximum altitude of the parabola trajectory.

The proposed terminal-angle constrained MPSP guidance law is applied for interceptor's midcourse flight. This approach requires the line-of-sight and line-of-sight rate information in real time. However, on-board detection system will not be activated until the capture conditions are satisfied. Assuming that the interceptor can receive target's information provided by ground radar or space-based infrared system, additional filter and prediction are necessary for signal extraction and denoising. For those air-breathing hypersonic targets, the interacting multiple model algorithm with commonly "CA" and "current" statistical models is preferred accounting for its complex maneuverability. However, it is reported in the literature that filter based on the nonlinear Markov acceleration model [34] exhibits better performance for boost-gliding targets.

Table 2: Convergence results of impact angle constrained guidance.

		$R(m)$	$\dot{q}(\mathrm{rad/s})$	$\theta_{\mathrm{imp}}(^\circ)$	$n_{yf}(g)$
$\theta_{\mathrm{imp}} = 170^\circ$	Default	60000	0	170	0.015
	Real	59981	$5.614e-6$	170.016	
$\theta_{\mathrm{imp}} = 180^\circ$	Default	60000	0	180	-0.051
	Real	59959	$-1.465e-5$	179.958	
$\theta_{\mathrm{imp}} = 190^\circ$	Default	60000	0	190	-0.104
	Real	59945	$-2.948e-5$	189.915	

In the terminal phase, the goal of guidance is trying to minimize the miss distance. However, the aerodynamic force in the near space is not enough. The reaction control system

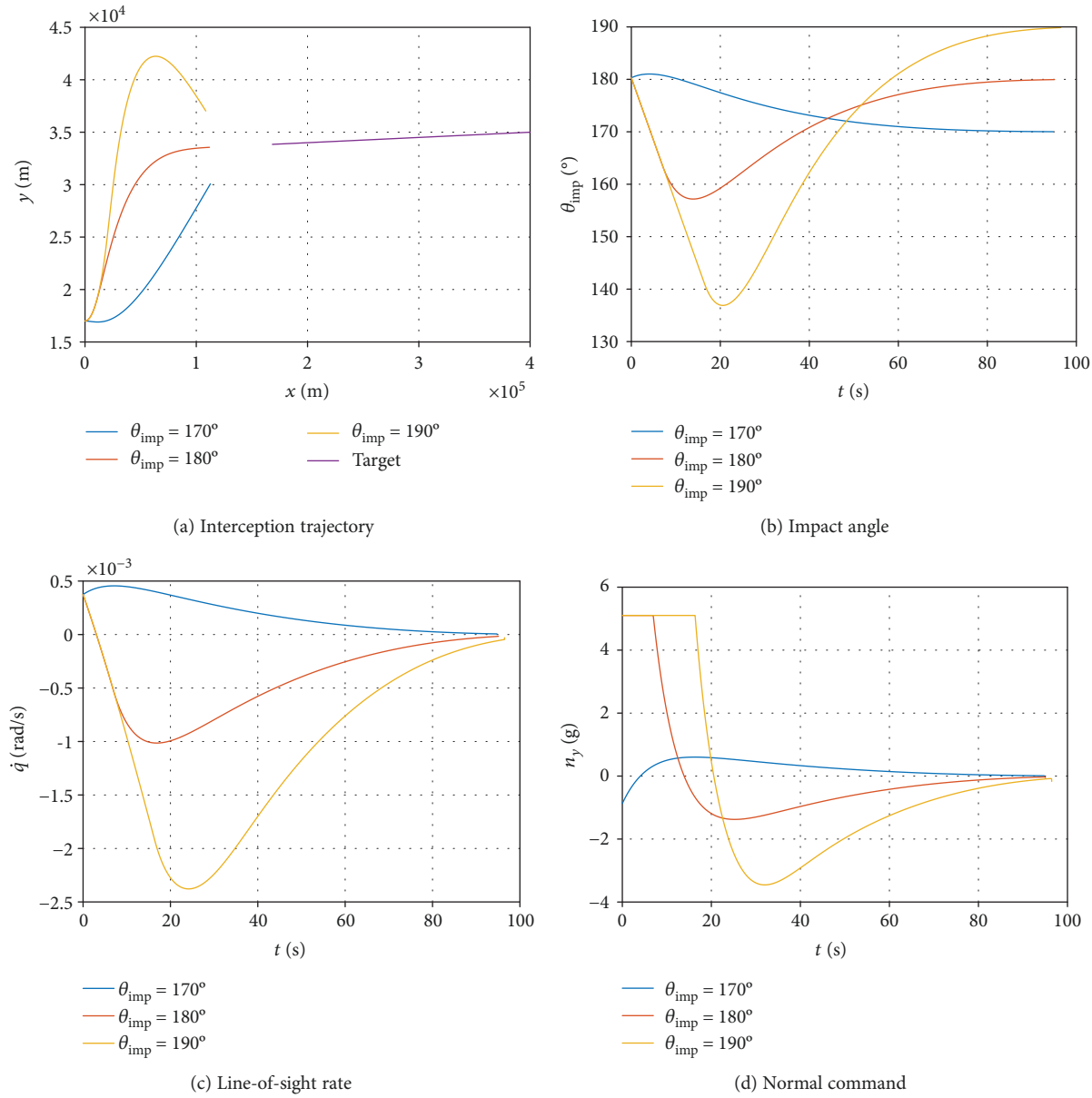

(a) Interception trajectory

(b) Impact angle

(c) Line-of-sight rate

(d) Normal command

FIGURE 4: Simulation results of impact angle constrained guidance.

is designed to accelerate the control response and increase the available overload. In addition, the on-board detection system is activated and target information is acquired without delay. Therefore, the guidance and control period has shortened obviously. For the above considerations, an analytic guidance called adaptive sliding mode guidance (ASMG) [35] is applied for terminal engagement, and the sign function is replaced by a saturation function to eliminate chattering. The acceleration command is expressed as

$$a_{M\varepsilon} = (k+1)\left|\dot{R}\right|\dot{q}_\varepsilon + \eta\frac{\dot{q}_\varepsilon}{|\dot{q}_\varepsilon| + \delta},$$
$$a_{MB} = (k+1)\left|\dot{R}_1\right|\dot{q}_\beta + \eta_1\frac{\dot{q}_\beta}{\left|\dot{q}_\beta\right| + \delta_1}. \quad (33)$$

where η, $\eta_1 > 0$, δ, and δ_1 are small positive scalars and $R_1 = R\cos(q_\varepsilon)$.

4.2. Line-of-Sight Constrained Guidance. Interception confrontation scenario is presented to verify the proposed line-of-sight constrained MPSP midcourse guidance. The following conditions are set assuming the adversaries are in the longitudinal plane.

(1) The initial position of the interceptor 0,17 km, the average velocity at 1200 m/s, 0° initial flight path angle, and 5 g maximum overload

(2) The initial position of hypersonic target 400,35 km, the average velocity at 2400 m/s, 180.286° initial flight path angle, and without maneuver

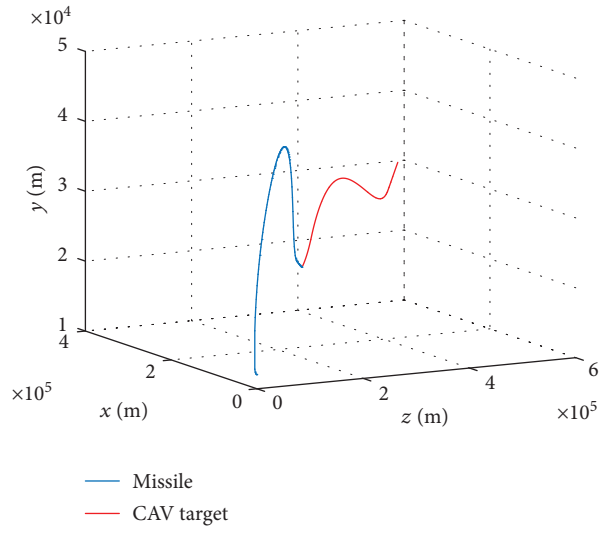

(a) Interception trajectory

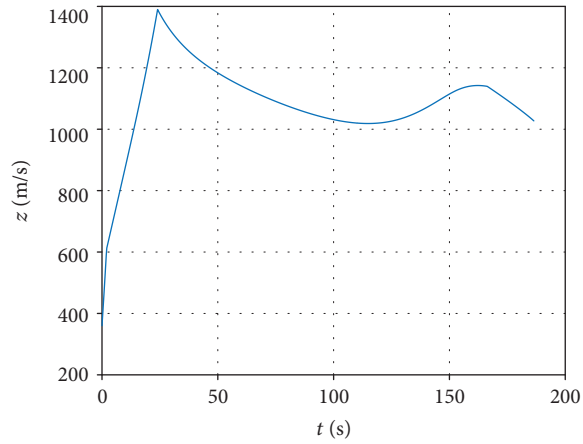

(b) Velocity

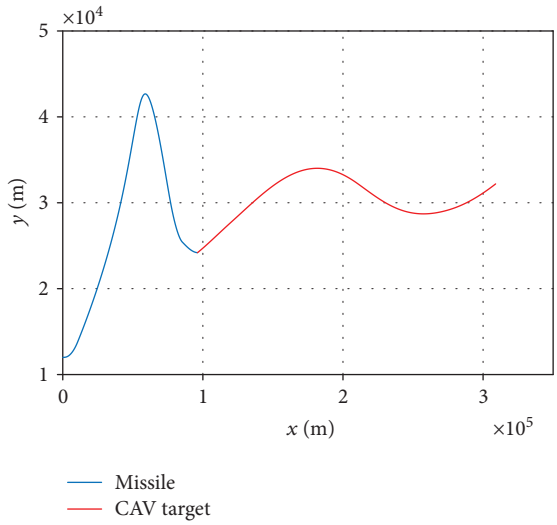

(c) Longitudinal trajectory

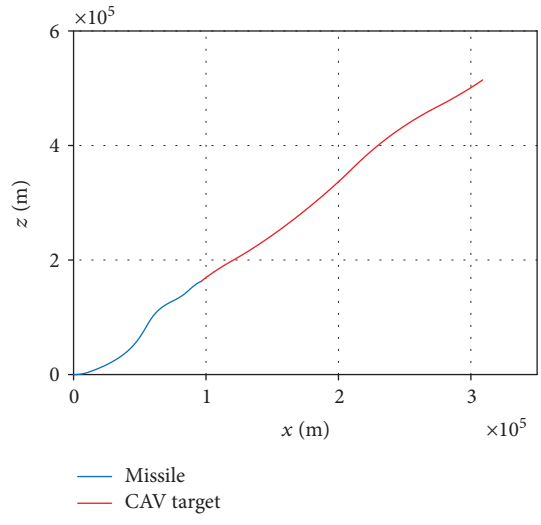

(d) Lateral trajectory

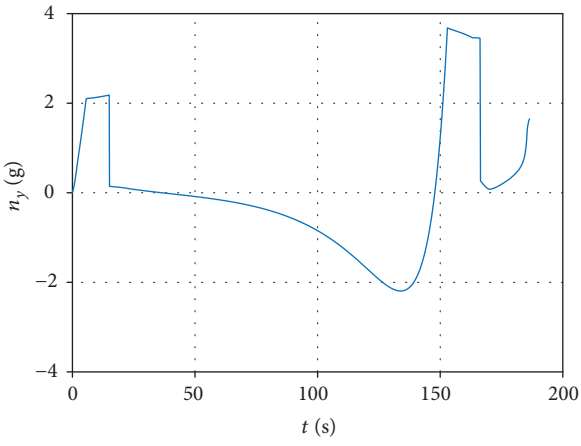

(e) Longitudinal load factor

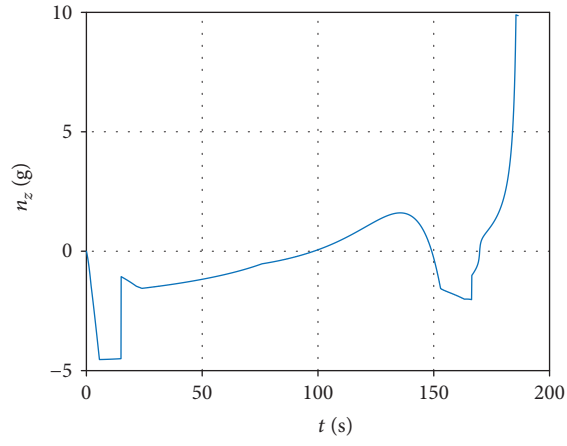

(f) Lateral load factor

Figure 5: Continued.

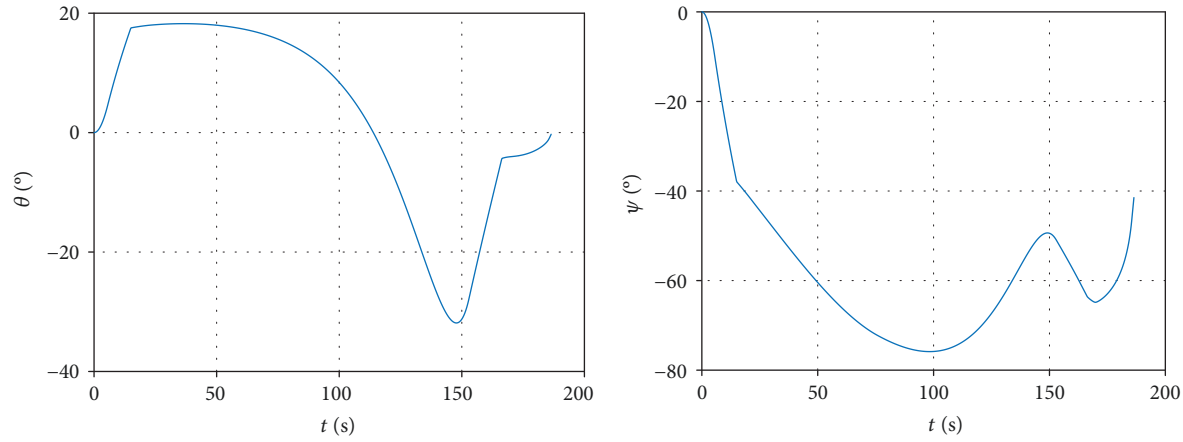

(g) Flight path angle

(h) Velocity azimuth angle

Figure 5: Simulation results of CAV interception.

(3) Terminal handover distance is 60 km, simulation step of 20 ms, and the scheduled final line-of-sights are -5°, 0°, and 5°, respectively

(4) Initial control guess utilizes the three-dimensional proportional guidance law

The results are shown in Table 1 and Figure 3.

From Figure 3(a), we can see that the interceptor is able to reach the desired position under the command of the line-of-sight constrained MPSP guidance algorithm, right in the front of the hypersonic target. Figures 3(a) and 3(b) indicate that the terminal constraints of both line-of-sight and line-of-sight rate have been satisfied with high accuracy. In Figure 3(d), the overload command can gradually converge to zero, thus providing a favorable initial condition for the endgame interception.

4.3. Impact Angle Constrained Guidance. To validate the impact angle constrained MPSP midcourse guidance, the same simulation conditions are set as in Section 4.2, except that the required impact angles are 170°, 180°, and 190°, where 180° represents a typical head-on collision. The simulation results are shown in Table 2 and Figure 4.

Similar conclusions can be made in contrast to the previous line-of-sight constrained MPSP guidance method. As shown in Figure 4(a), the interceptor is able to reach the desired position under the command of the impact angle constrained MPSP guidance algorithm. Figures 4(b) and 4(c) imply that the terminal constraints of both impact angle and line-of-sight rate have been satisfied. In Figure 4(d), the overload command gradually converges to zero and therefore provides a favorable initial condition for the endgame interception.

4.4. Full Trajectory Interception. To verify the effectiveness of full trajectory guidance scheme, parameters are set as follows:

(1) Initial position of interceptor is 0,12,0 km, initial velocity is 360 m/s, and initial flight path angle and velocity azimuth angle are both 0°

(2) The interceptor's rocket works in two levels, the first level lasts 2 s and produces 30kN thrust, while the second level lasts 22 s and produces 8 kN thrust

(3) The hypersonic target maintains pullup and pull-down gliding trajectory with an initial altitude of 60 km and speed of 5100 m/s

Assuming that the interceptor is released once the missile-target range meets the desired distance, simulation results are shown in Figure 5. From that, we can see the progress of the interceptor. After launching from an airborne platform, the interceptor climbs to upper air under trigonometric guidance. Until 15.00 s later, it turns to midcourse phase and keeps accelerating. A maximum speed of 1389.92 m/s is achieved when the rocket engine burns out at 24.00 s. The trajectory reaches a maximum altitude of 42.67 km after 113.36 s. Separation from booster rocket appears at 166.33 s when the handover range is reached and terminal guidance takes over. The final miss distance is 2.47 m after 186.44 s flight, which demonstrates the correctness of the proposed guidance strategy.

5. Conclusions

This paper proposes a novel midcourse guidance strategy for interceptors against near-space hypersonic targets. The characteristics of hypersonic weapon defense and the requirements of midcourse guidance design for interceptors are analyzed. The line-of-sight coupled interception model is established in a three dimensional space. Under the assumption that the closing velocity remains constant and the target maneuver is briefly negligible, a MPSP method-based suboptimal midcourse guidance law is derived for two different purposes that either satisfies the terminal line-of-sight angle constraint or satisfies the terminal impact angle constraint. Results indicate that the designed angle can be realized with maximum error less than 0°. In addition, the line-of-sight rate approaches zero at handover time, which implies that the final overload command can converge to a small value. In the interception of a hypersonic gliding target, the final

miss distance turns out to be 2.47 m, which proves the effectiveness of this guidance law.

Data Availability

The data used to support the findings of this study are available from the corresponding author upon request.

Conflicts of Interest

The authors declare that they have no conflicts of interest.

Acknowledgments

This research was supported by the National Natural Science Foundation of China (Grant no. 61503301) and the National Safety Academic Fund (Grant no. U1630127).

References

[1] J. J. Spravka and T. R. Jorris, "Current hypersonic and space vehicle flight test instrumentation challenges," in *AIAA Flight Testing Conference, AIAA AVIATION Forum*, pp. 1–15, Dallas, TX, USA, 2015.

[2] K. Reif, "Hypersonic advances spark concern," *Arms Control Today*, vol. 48, no. 1, pp. 29-30, 2018.

[3] J. Fisher and D. Richard, "US confirms sixth Chinese hypersonic manoeuvring strike vehicle test," *Jane's Defence Weekly*, vol. 52, no. 48, 2015.

[4] J. Drew, "DARPA confident of current U.S. hypersonic missile path," *Aerospace Daily and Defense Report*, vol. 257, no. 52, 2016.

[5] B. Sridhar and N. K. Gupta, "Missile guidance laws based on singular perturbation methodology," *Journal of Guidance Control and Dynamics*, vol. 3, no. 2, pp. 158–165, 1980.

[6] D. S. Naidu and A. J. Calise, "Singular perturbations and time scales in guidance and control of aerospace systems: a survey," *Journal of Guidance Control and Dynamics*, vol. 24, no. 6, pp. 1057–1078, 2001.

[7] M. Manickavasagam, A. K. Sarkar, and V. Vaithiyanathan, "A singular perturbation based midcourse guidance law for realistic air-to-air engagement," *Defence Science Journal*, vol. 67, no. 1, pp. 108–118, 2016.

[8] N. Indig, J. Z. Ben-Asher, and N. Farber, "Near-optimal spatial midcourse guidance law with an angular constraint," *Journal of Guidance, Control, and Dynamics*, vol. 37, no. 1, pp. 214–223, 2014.

[9] X. Liu, S. Tang, J. Guo, Y. Yun, and Z. Chen, "Midcourse guidance law based on high target acquisition probability considering angular constraint and line-of-sight angle rate control," *International Journal of Aerospace Engineering*, vol. 2016, Article ID 7634847, 20 pages, 2016.

[10] M.-G. Seo and M.-J. Tahk, "Suboptimal mid-course guidance algorithm for accelerating missiles," *Proceedings of the Institution of Mechanical Engineers, Part G: Journal of Aerospace Engineering*, vol. 231, no. 11, pp. 2032–2047, 2017.

[11] C. A. Phillips and J. C. Drake, "Trajectory optimization for a missile using a multitier approach," *Journal of Spacecraft and Rockets*, vol. 37, no. 5, pp. 653–662, 2000.

[12] S. Jalali-Naini and S. Pourtakdoust, "Modern midcourse guidance laws in the endoatmosphere," in *AIAA Guidance, Navigation, and Control Conference and Exhibit*, pp. 1–17, San Francisco, CA, USA, 2005.

[13] R. Jamilnia and A. Naghash, "Optimal guidance based on receding horizon control and online trajectory optimization," *Journal of Aerospace Engineering*, vol. 26, no. 4, pp. 786–793, 2013.

[14] P. N. Dwivedi, A. Bhattacharyya, and R. Padhi, "Computationally efficient suboptimal mid course guidance using model predictive static programming (MPSP)," *IFAC Proceedings Volumes*, vol. 41, no. 2, pp. 3550–3555, 2008.

[15] P. N. Dwivedi, A. Bhattacharya, and R. Padhi, "Suboptimal midcourse guidance of interceptors for high-speed targets with alignment angle constraint," *Journal of Guidance, Control, and Dynamics*, vol. 34, no. 3, pp. 860–877, 2011.

[16] R. Padhi and M. Kothari, "Model predictive static programming: a computationally efficient technique for suboptimal control design," *International Journal of Innovative Computing, Information and Control*, vol. 5, no. 2, pp. 399–411, 2009.

[17] H. B. Oza and R. Padhi, "Impact-angle-constrained suboptimal model predictive static programming guidance of air-to-ground missiles," *Journal of Guidance, Control, and Dynamics*, vol. 35, no. 1, pp. 153–164, 2012.

[18] O. Halbe, R. G. Raja, and R. Padhi, "Robust reentry guidance of a reusable launch vehicle using model predictive static programming," *Journal of Guidance, Control, and Dynamics*, vol. 37, no. 1, pp. 134–148, 2014.

[19] N. G. Bhitre and R. Padhi, "State constrained model predictive static programming: a slack variable approach," *IFAC Proceedings Volumes*, vol. 47, no. 1, pp. 832–839, 2014.

[20] K. Sachan and R. Padhi, "Fuel-optimal G-MPSP guidance for powered descent phase of soft lunar landing," in *2015 IEEE Conference on Control Applications (CCA)*, pp. 924–929, Sydney, Australia, 2015.

[21] S. Li and X. Li, "Sub-optimal sliding mode guidance law based on MPSP," *Flight Dynamics*, vol. 34, no. 5, pp. 54–58, 2016.

[22] A. Maity, H. B. Oza, and R. Padhi, "Generalized model predictive static programming and angle-constrained guidance of air-to-ground missiles," *Journal of Guidance, Control, and Dynamics*, vol. 37, no. 6, pp. 1897–1913, 2014.

[23] A. Maity, R. Padhi, S. Mallaram, G. M. Rao, and M. Manickavasagam, "A robust and high precision optimal explicit guidance scheme for solid motor propelled launch vehicles with thrust and drag uncertainty," *International Journal of Systems Science*, vol. 47, no. 13, pp. 3078–3097, 2016.

[24] P. Kumar, A. Bhattacharya, and R. Padhi, "MPSP guidance of tactical surface-to-surface missiles with way-point as well as terminal impact and body angle constraints," in *2013 IEEE International Conference on Control Applications (CCA)*, pp. 865–870, Hyderabad, India, 2013.

[25] H. Guo, W. Fu, B. Fu, K. Chen, and J. Yan, "Penetration trajectory programming for air-breathing hypersonic vehicles during the cruise phase," *Journal of Astronautics*, vol. 38, no. 3, pp. 287–295, 2017.

[26] T. Shima and O. M. Golan, "Head pursuit guidance," *Journal of Guidance, Control, and Dynamics*, vol. 30, no. 5, pp. 1437–1444, 2007.

[27] O. M. Golan and T. Shima, "Head pursuit guidance for hypervelocity interception," in *AIAA Guidance, Navigation, and Control Conference and Exhibit, Guidance, Navigation, and Control and Co-located Conferences*, pp. 1–12, Providence, RI, USA, 2004.

[28] A. Lele, *Hypersonic Weapons*, Institute for Defence Studies and Analyses, 2017.

[29] L. Zhou, *Analysis of encounter conditions for intercepting a hypersonic target [M.S. thesis]*, Harbin Institute of Technology, 2016.

[30] K. Ma and X. Zhang, "A novel guidance law with line-of-sight acceleration feedback for missiles against maneuvering targets," *Mathematical Problems in Engineering*, vol. 2014, Article ID 983751, 8 pages, 2014.

[31] S. R. Kumar, S. Rao, and D. Ghose, "Sliding-mode guidance and control for all-aspect interceptors with terminal angle constraints," *Journal of Guidance, Control, and Dynamics*, vol. 35, no. 4, pp. 1230–1246, 2012.

[32] P. Lu, "Entry guidance: a unified method," *Journal of Guidance, Control, and Dynamics*, vol. 37, no. 3, pp. 713–728, 2014.

[33] X. R. Yang, J. H. Liang, and X. D. Li, "Study on parabola-trajectory simulation of air-to-air missile," *Journal of System Simulation*, vol. 22, no. 5, pp. 1261–1265, 2010.

[34] M. E. Hough, "Reentry maneuver estimation using nonlinear Markov acceleration models," *Journal of Guidance, Control, and Dynamics*, vol. 40, no. 7, pp. 1693–1710, 2017.

[35] D. Zhou, *New Guidance Laws for Homing Missile*, National Defense Industry Press, 2002.